NUMERICAL STUDY OF SPHERICAL INDENTATION IN SUPERFICIAL COATINGS

Avelino Manuel da Silva Dias*
Federal University of Rio Grande do Norte (UFRN), Mechanical Department, Campus Universitário, s/n – Lagoa Nova – Natal – RN 59072-970, Brazil

ABSTRACT

The aim of this work was to simulate the indentation testing behaviour of a rigid ball indenter on a coating/substrate system by the finite element method. Indentation testing has been used for a long time to determinate the superficial hardness of different materials. Nowadays, a number of researchers have developed new techniques based on this testing to evaluate different mechanical properties of materials including fracture toughness and Young modulus. However, there are still limitations to analyze the coating/substrate system behaviour during indentation testing. To help to reduce those limitations, the present work uses the finite element technique to simulate stress and strain fields during the indentation cycle. A commercial finite element code which has been considered as a promising tool for non linear problems and fracture process was used. The numerical results for the stress and strain fields focused mainly in the indenter contact region and for interface between coating and substrate were calculated during the testing cycle. Furthermore, through the use of the maximum principal stress criterion, details of the failure mechanism that occurs on coating system were evaluated.

Keywords: *Finite Element, Indentation Testing, Thin Films, Contact.*

1. INTRODUCTION

Recently, indentation testing's have been used as a potential tool to evaluate mechanical characteristics of materials including, for example, the Young modulus (E), the Poisson coefficient (ν) and also the elastic-plastic behaviour curve [1-3]. However, the implementation of this indentation technique to obtain different mechanical properties does still bring many doubts to the scientific community. These doubts are particularly stronger when the testing procedure is used to evaluate the mechanical behaviour of hard thin films applied over soft metal substrates. The limitations of this testing procedure have triggered, the use of numerical techniques to simulate it, including the calculation of the stress and strain fields during the indentation cycle, to allow a more reliable interpretation of it.

In the last few years, a great volume of research work has been developed to evaluate the behaviour of different material classes during indentation testing with numerical techniques [4-11]. On the other hand, the use of numerical techniques to study the indention testing on thin superficial coatings has also presented several problems mainly associated to the difficulty to characterize these coatings, to establish and implement failure criteria, and, mainly, to obtain reliable mechanical properties of the coating/substrate system. Furthermore, computational limitations are also indicated as difficulties to simulate de indentation testing [4, 10, 12-13].

Plastic deformation is a major concern in the design and performance of engineering components. Failure of a hard coating deposited in a soft substrate under many tribological situations is seldom caused by conventional wear but by debonding of the coating from the substrate (adhesive failure), or fracture of the coating (cohesive failure), or even by subsurface fracture (substrate failure). Accordingly, it is imperative to determine the distribution of the plastic strain and the beginning of the plastic zone, so as to have a better understanding of the mechanisms of surface and subsurface wear involving localized plastic flow [4, 13].

In an attempt to comprehend the mode of deformation of a surface coating during the indentation cycle with a spherical indenter, Vanimisetti and Narasimhan [10] published results from a numerical analysis of the test of a thin hard film deposited on a soft substrate. The authors analysed the film stress distribution and identified a transition of this stress field during the testing, which varied from a contact stress field to flexure stress in the beginning of the testing. Moreover, depending on the indentation depth, the film stress field behaved as membrane stress with tension stresses on both circumferential and radial directions. The authors evaluated the influence of the system (coating and substrate) strength and the presence of residual stresses on the indentation response. Finally, they present an initial study of fracture process that occurs in this system during the indentation testing.

More recently, different authors have proposed new methods for determining the mechanical properties of thin films by combining experimental instrumented indentation testing with the finite element analysis. In all these works the authors draw attention to the need for a careful analysis of the results of the numerical behaviour of the stress and strain fields. The relationship between the depths of penetration of the indenter with the film thickness is another important point for validation of these new methodologies for studies coating/substrate system found in the literature [3, 11, 12].

The proposed simulations of this work were performed using the Finite Element Method (FEM) on a commercial solver [14]. The FEM has been greatly used to simulate and solve many non-linear problems in different areas like structural instability, dynamic, fluid and electromagnetic systems, and mechanical forming and fracture process. The principal aim of this work was to evaluate the contact stress and strain fields during the indention testing with rigid spherical indenter on coating/substrate systems with different penetration depths. It were analysed four monolayer systems produced by plasma deposition (PVD), recovered of Chromium Nitrate (CrN) with different thickness on two metal substrates. One of them was considered soft substrate and the other was a hard substrate.

2. METHODOLOGY

The indentation testing consist of a penetration an indenter, which may, in most cases, considered a rigid body, on the surface of a sample of the analysed material [3]. For the simulation of this test with a spherical indenter, the symmetry of the problem was considered and the axis-symmetric elements were used in the model, which greatly reduced the complexity and computational effort need to analyze the problem.

The numerical simulation of the indentation cycle, including both loading and unloading steps, presented in this work, used a prescribed displacement scheme to guarantee a better control in the beginning and during all the indentation cycle [3]. This procedure is consistent with experimental indentation testing, since the indenter displacement is applied with a small penetration speed and the behaviour of the load in function of displacement is obtained by the load sensor installed on the indenter table. Besides this numerical control, the simulation was developed in two phases, one related to the indenter coming down, followed by its coming up, and the completing the cycle [9]. The Pile-up and sinking-in surface displacements, which can occur during the testing, were not taken into consideration in this work. Likewise, the friction coefficient between the indenter and the sample was considered to be zero, because there is some evidence that this friction do not interfere with the numerical results [2, 9, 13]. To improve the results of the stress distribution in the indenter contact region and in the interface between coating and substrate, a more refined mesh were used in these regions, figure 1.

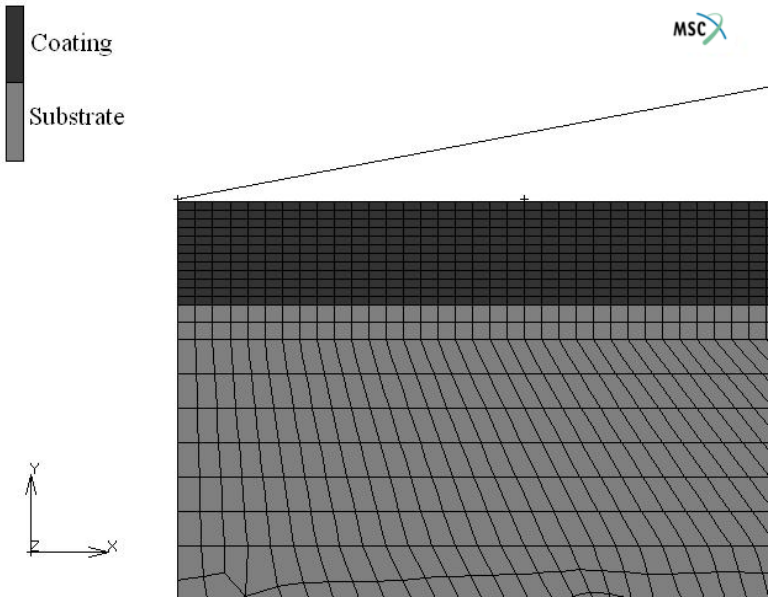

Figure 1. Detail of the numerical model mesh close to the indentation area.

In present analysis, the spherical indenter was modelled as a rigid semicircular shell, with three different diameters which penetrates in the sample of the studied systems. It was considered that a perfect adherence exists between the coating and the substrate. The boundary conditions included a displacement restriction that was imposed to the base of the sample and radial displacement restriction to the nodes localized in the axis of symmetry [4, 13]. During the simulation, two hundreds increments were used to represent the loading of the indenter and one hundred to model its removal from the sample, completing the indentation cycle.

Different systems, composed by monolayer coatings of *CrN*, with two different thicknesses (t), and two steel substrates, a hard metallic substrate and a soft one, were simulated. For the system with thicker film (t = 15 µm), 1036 isoperimetric axis-symmetric elements with eight nodes were used, being 460 elements were used to represent

the film and the remainder for the substrate. On the other hand, for the sample with smaller thickness film (t = 5 μm), it was only 806 elements with eight nodes.
The adopted penetration depth (h_{max}) was 1,5 μm for the systems with smaller thickness and varied from 2.5 μm to 7.5 μm for the system with bigger thickness. Those penetrations values were based on results from tests performed in an instrumented ultra-microhardness equipment [15].

Table 1 shows the mechanical properties of the materials that were used in this work. These values were founded in the specialized literature. Both the coating and the substrate materials were considered isotropic and homogeneous. The following models for the elastic-plastic behaviour of the system were adopted: the CrN film was considered as perfectly plastic [4]; the hard substrate steel was represented through an elastic-plastic flow curve [9] and the behaviour of soft substrate was represented by a stress in function of strain curve obtained on the finite element solver library [14].

Table 1. Mechanical properties of the materials used in this work [15-16].

Material	Young Modulus (E)	Poisson Coefficient (ν)	Yield Strength (σ_y)
Coating (CrN)	380 GPa	0.22	4000 MPa
Hard steel substrate (AISI 301)	195 GPa	0.30	1900 MPa
Soft steel substrate (SAE 1045)	217 GPa	0.30	400 MPa

3. TESTING THE NUMERICAL MODEL

The validity of the numerical model had been tested by comparing the finite element results for the uncoated sample and the rigid ball with the results of analytical Hertz solution, eq. (1). In this expression, a was the contact area radius, F was the force and R was the radius of the indenter. In this procedure, a linear elastic analysis was adopted. The numerical result of the contact area was compared to the result obtained by Eq. (1) for a contact between a rigid sphere and a semi-infinite plate [16].

$$a = \sqrt[3]{\frac{3FR}{E^*}} \tag{1}$$

$$E^* = \frac{E}{(1-\nu^2)} \tag{2}$$

Applying eq. (1) and eq. (2) to the contact between a spherical indenter with a hundred micrometer radius with a metallic hard substrate (E = 195 GPa and ν = 0.30), it was obtained the analytical value for the elastic contact radius a, which presented a difference of 5.3% when compared to the value obtained numerically. This simple procedure demonstrated that the numerical model was able to represent well the contact between the indenter and the sample and the stress gradient in the contact region.

4. RESULTS AND DISCUSSIONS

Table 2 compares the indentation force obtained for different systems by the simulation analysis. As the simulation was performed by imposing a prescribed maximum displacement to the indenter (h_{max}), different indentation forces were obtained according to the mechanical properties of each system. The results indicate that, for similar systems, those with a thicker coating required a larger force during indentation. On the other hand, when different systems were compared, those with a hard substrate needed a larger indentation force. Also, as expected, the penetration force increased if the penetration depth was increased for the same system.

Table 2. Calculated indenter force for different monolayer systems.

System	Diameter indenter	Thickness of film	Indentation depth	Ratio $t \times h_{max}$	Indenter force
CrN-SAE 1045	200 μm	5 μm	1.5 μm	0.300	30.1 N
		15 μm	2.5 μm	0.167	51.8 N
	100 μm	15 μm	2.5 μm	0.167	47.3 N
			5.0 μm	0.333	60.3 N
			7.5 μm	0.500	69.2 N
	1.0 mm	15 μm	2.5 μm	0.167	52.9 N
			5.0 μm	0.333	103.8 N
			7.5 μm	0.500	123.2 N
CrN-AISI 301	200μm	5 μm	1.5 μm	0.300	58.8 N
		15 μm	2.5 μm	0.167	102.5 N
	100 μm	15 μm	2.5 μm	0.167	87.6 N
			5.0 μm	0.333	123.9 N
			7.5 μm	0.500	139.7 N
	1.0 mm	15 μm	2.5 μm	0.167	116.7 N
			5.0 μm	0.333	209.8 N
			7.5 μm	0.500	248.2 N

The calibration procedure of the numerical model and these first results of the indenter force showed that qualitatively the implemented simulations were able to represent some characteristics of the global behaviour of these indentation essays of the *CrN* monolayer system in two different metallic substrates.

Figure 2 presents the numerical results of the plastic strain for the testing using an indenter with one millimetre radius and a penetration depth of five micrometer. This graphic shows the behaviour of this strain for the system *CrN* on hard steel substrate with the 15 μm thickness film. For illustrating this behaviour during the indentation cycle it was chosen four nodes: two of them located in the coating, the first one (node four) in the middle of the film and the second near the interface with the substrate (node 907). The others two nodes were situated in the substrate (node nine and node 909), both next to the interface between coating and substrate. In this simulation, the penetration depth corresponded to one third of the film thickness and, in function of the contact area between indenter and the sample, a gradient of bending stress occurred in the coating during this testing.

Comparing the result of figure 2 to the ones obtained for the film of smaller thickness, it was verified that the systems with higher thickness coating presented a lower intensity in the plastic strain field. Likewise, it was verified that the interface region were submitted to highest stress gradients for the system whose ratio between penetration depth and film thickness was bigger. In the specialized literature when there is formation of two plastic zones, one in the substrate and another in the coating, during indentation cycle, the thickness of the film and the mechanical strength of the substrate were high enough to protect the system of a possible delamination [4]. The numerical result for the system showed in figure 2 (*CrN* with fifteen micrometres thickness deposited in hard substrate) indicated that this system could be protected of a possible delamination in service.

Figure 3 shows the numerical distribution of the indentation essay in a system CrN on soft steel substrate with 15 μm thickness film. In this other procedure, the indenter had one millimetre radius and the depth penetration was five micrometer. The three nodes identified in this graphic were situated in the film, the first one near the film surface (node two), the second in the middle of the coating (node four) and the third one next to the interface with substrate (node six). Evaluating the normal stress in these points, it was possible to verify a change in the behaviour of the stress gradient during the indentation cycle. Initially, this stress field was originated by the contact between the indenter and the sample, in a second moment, this gradient became to the bending stress. Finally, at the end of the loading phase, this stress begun to having a membrane behaviour. This numerical result also shows that at the end of the essay, the coating had a residual tension stress field. This change in the stress gradient during the indentation testing was observed in literature [10]. They correlated this behaviour with the ratio between the penetration depth and the contact area of the indenter. Similar behaviours of these stress fields occurred in the simulations with others systems and were more intense in the systems with thinner thickness of the film and in those submitted to highest penetration depth.

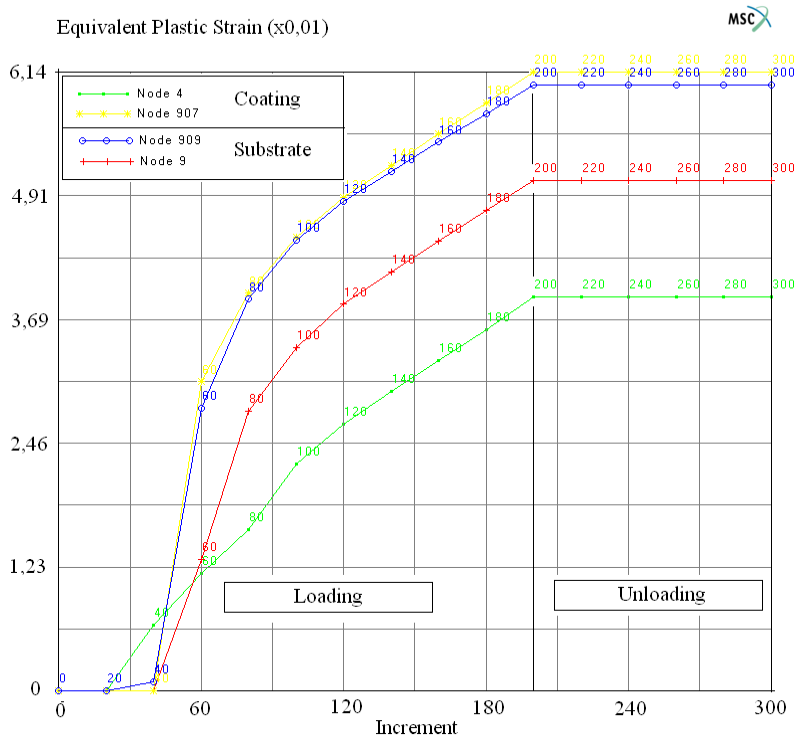

Figure 2. Numerical evaluation of plastic strain during indentation cycle for the CrN film with 15 µm thickness.

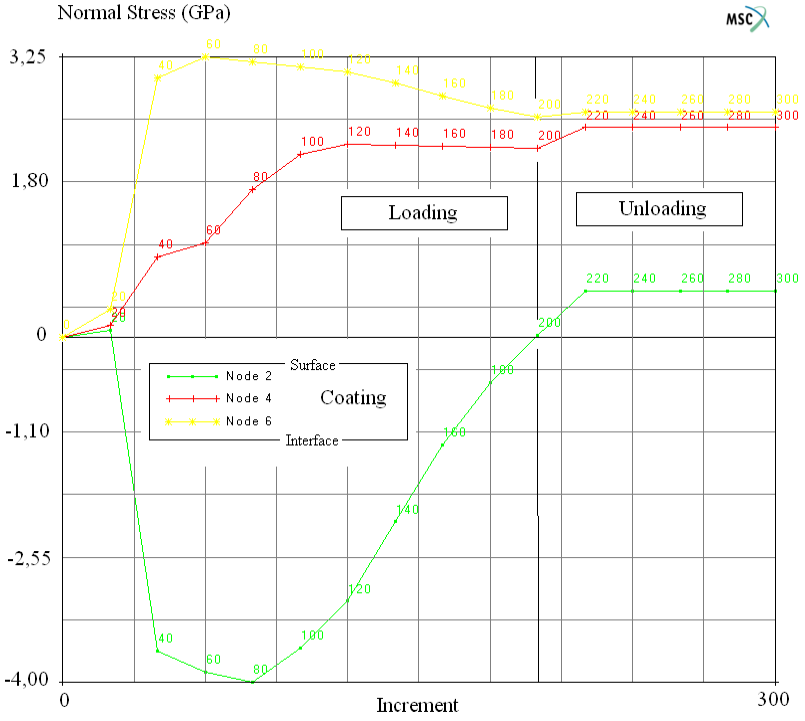

Figure 3. Numerical evaluation of normal stress in coating during indentation testing.

In experimental testing of films with spherical indenters is more common the arising of circular and radial cracks around the indentation impression. Figure 4 presents the top view impression of a spherical indenter in the surface of CrAlN film deposited in stainless steel substrate by PVD process [15]. In this figure is possible to visualize the superficial circular cracks around the indentation impression.

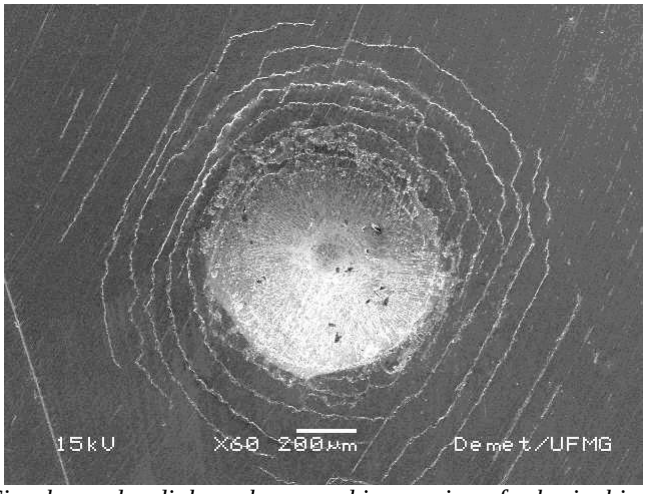

Figure 4. Circular and radial cracks around impression of spherical indenter [15].

Figure 5 shows the numerical distribution obtained for the highest principal stress in the radial direction of the contact between the indenter and the specimen. This simulation have been used the system with *CrN* film with 15 µm thickness deposited in soft substrate (SAE 1045). Considering the *CrN* film as a brittle material and adopting the highest principal stress theory as a failure criterion, it was possible to identify a critical region in the surface of the system near the indenter impression and another near to the interface with the substrate. The level of this numerical stress reached values as near as the film yielding limit, as showed in table 2. These numerical results demonstrating how these two regions were critical like the experimental results in similar systems. These critical regions were also identified in the others systems studied in this present work. By that, it was opted to analyzing the behaviour of three points at these regions during the indentation cycle for the others two systems.

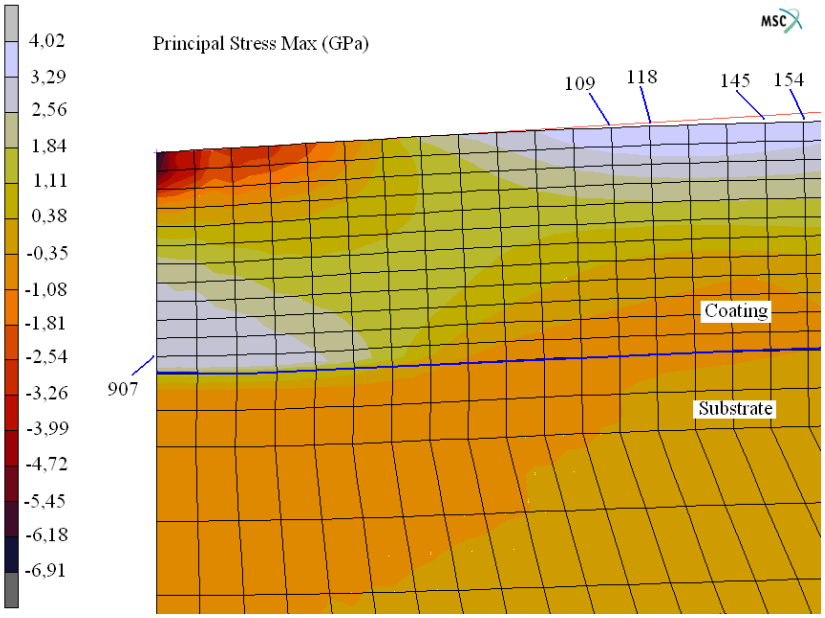

Figure 5. The Maximum Principal Stress distributions in the contact area of the indenter.

Figure 6 presents the behaviour of the highest principal stress during the indentation cycle for the *CrN* with 15 µm of film thickness deposited in hard substrate. It was verified that for the nodes situated in the film surface, the maximum principal stress reached a landing of 3.67 GPa, near the yielding limit of the *CrN* coating. These numerical results were compatible with experimental observations made indentation testing of thin hard films. On the order hand, for the node 907, situated near the substrate interface, the maximum principal stress level was around 1.80 GPa and its tension behaviour during all indentation cycle also showed that this system could be protected of a possible delamination in service.

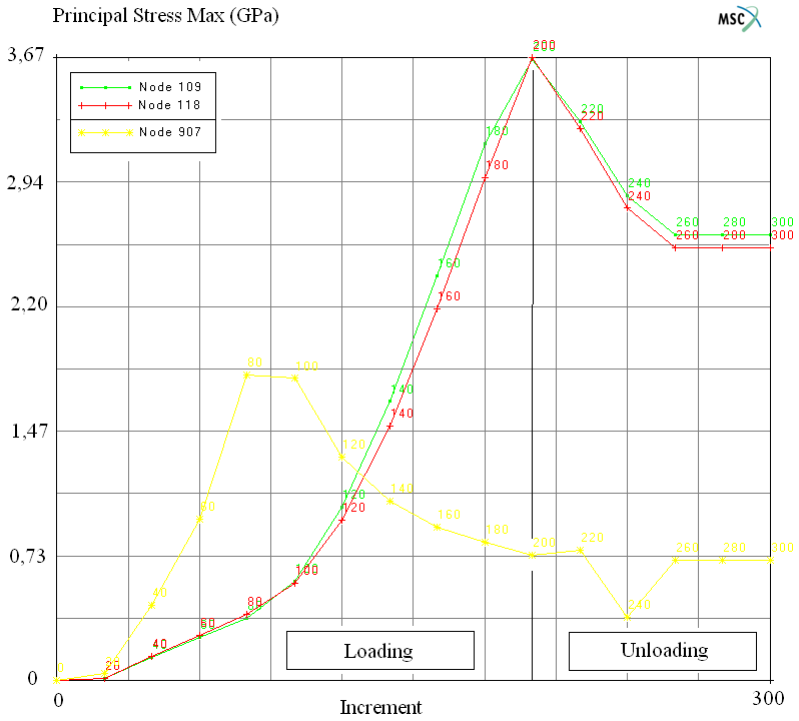

Figure 6. Numerical evolution of highest principal stress during indention in CrN with fifteen micrometres thickness deposited in hard substrate.

Figure 7 also shows the behaviour of the maximum principal stress during the indentation cycle but in this moment for the system *CrN* with fifteen micrometres thickness deposited in soft substrate. Once again, the maximum principal stress at the nodes situated in the film surface reached levels near the *CrN* yielding limit (σ_{1max} = 4.02 GPa). For the node situated next to the substrate interface, the level of the maximum principal stress (σ_{1max} = 3.40 GPa) also was near the coating limit and this tension behaviour during all cycle also showed that this was a critical area. Comparing this graphic results with the previous system (*CrN* – hard substrate), it was observed that the gradient stress was bigger in the system that the substrate had lower mechanical strength. This numerical observation was compatible with experimental studies obtained in the specialized literature. Finally, for this last system analyzed, the level of the maximum principal stress in the region of substrate interface had to be taken into consideration as this indicated a possible coating delamination in service.

5. CONCLUSIONS

Based in the numerical results of the indentation essay with spherical indenter in different systems, through the finite element method, it was possible to present the following conclusions:

• The numerical model obtained was capable to well represent the contact between the indenter and the sample when compared with the analytical Hertz solution;

• In the global behaviour viewpoint, the models were able to represent satisfactorily the indentation testing in different composed systems CrN, with different thicknesses, deposited in two different metallic substrates;

• It was evaluated the stresses numerical evolutions during the indentation cycle for the studied systems. The gradient stress behaviour showed a change in this field, passing from a contact stress to bending stress and, in some cases, finishing like a membrane stress. In the evaluation of the plastic strain for the thicker coating system, it was verified the formation of two plastic regions, one in the coating and another in the substrate;

• The numerical analysis of critical regions to cracking using the highest principal stress theory as failure criterion showed compatible with the fissures obtained experimentally, in the testing with spherical indenters.

• Moreover, in the view the highest principal stress theory, numerical results identified a possible delamination in some studied systems, like the systems with thin thickness coatings and also in the systems with soft substrate;

• It is also necessary a deep analysis of these numerical procedures to better identify the delamination and fracture process in the coating (cohesive failure), as well as, failure in the substrate (sub-superficial fracture);

• Furthermore, it is important to implement essays for the mechanical proprieties obtaining for a coating/substrate system and so better represent them numerically.

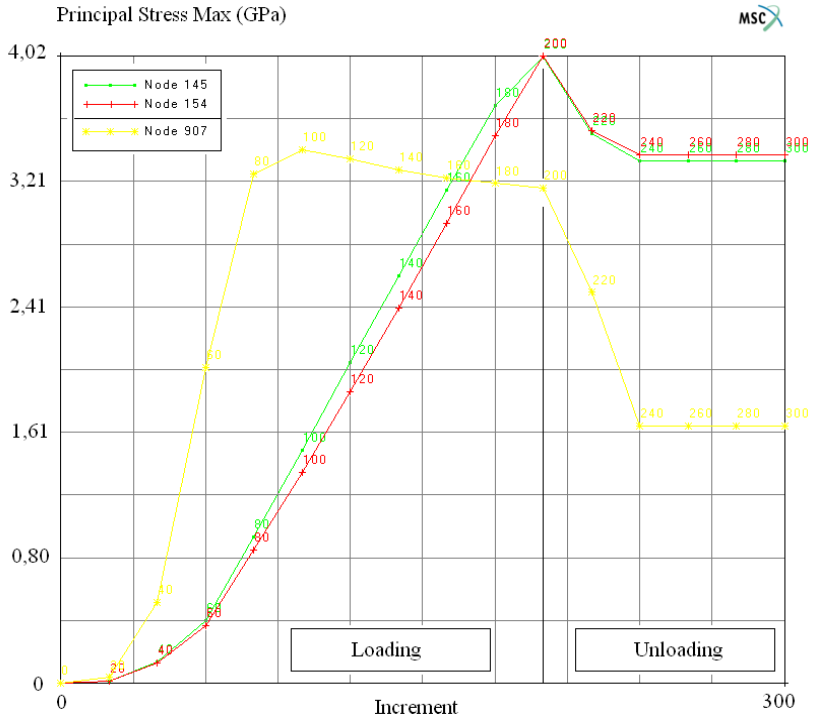

Figure 7. Numerical evolution of highest principal stress during indention testing in CrN with fifteen micrometres thickness deposited in soft substrate.

6. ACKNOWLEDGEMENTS

The present work was supported by FAPEMIG (Foundation for the Support of Research in the State of Minas Gerais) and CNPq (Brazilian Research Council).

7. REFERENCES

[1]. K. Zeng, C. Chiu, 2001, An Analysis of Load-Penetration Curves from Instrumented Indentation, *Acta Materialia*, **49**, 3539-3551 (2001).
[2]. H. Lee, J. H. Lee, G. M. Pharr, A Numerical Approach to Spherical Indentation Techniques for Material Property Evaluation, *Journal of the Mechanics and Physics of Solids*, **53**, 2037-2069 (2005).
[3]. A. M. S. Dias, G. C. D. Godoy, Determination of Stress-Strain Curve through Berkovich Indentation Testing, *Materials Science Forum*, **636-637**, 1186-1193 (2010).
[4]. Y. Sun, A. Bloyce, T. Bell, Finite Element Analysis of Plastic Deformation of Various TiN Coating/Substrate Systems under Normal Contact with a Rigid Sphere, *Thin Solid Films*, **271**, 122-131 (1995).
[5]. R. M. Souza, G. G. W. Mustoe, J. J. Moore, Finite Element Modelling of the Stresses, Fracture and Delamination During the Indentation of Hard Elastic Films on Elastic-Plastic Soft Substrates, *Thin Solid Films*, **392**, 65-74 (2001).
[6]. A. Carpinteri, B. Chiaia, S. Invernizzi, Numerical Analysis of Indentation Fracture in Quasi-brittle Materials, *Engineering Fracture Mechanics*, **71**, 567-577 (2004).
[7]. L. A. Piana, R. E. A. Pérez, R. M. Souza, A. O. Kunrath, T. R. Strohaecker, Numerical and Experimental Analyses on the Indentation of Coated Systems with Substrates with Different Mechanical Properties, *Thin Solid Films*, **491**, 197-203 (2005).
[8]. J. M. Antunes, L. F. Menezes, J. V. Fernandes, Three-dimensional Numerical Simulation of Vickers Indentation Testing, *International Journal of Solids and Structures*, **43**, 784-806 (2006).
[9]. A. M. S. Dias, P. J. Modenesi, G. C. D. Godoy, Computer Simulation of Stress Distribution During Vickers Hardness Testing of WC-6Co, *Materials Research*, **9**, Issue 1, 73-76 (2006).
[10]. S. K. Vanimisetti, R. Narasimhan, A Numerical Analysis of Spherical Indentation Response of Thin Hard Films on Soft Substrates, *International Journal of Solids and Structures*, **43**, 6180-6193 (2006).
[11]. S. A. R. Pulecio, M. C. M. Farias, R. M. Souza, Finite element and dimensional analysis algorithm for the prediction of mechanical properties of bulk materials and thin films, *Surface & Coatings Technology*, **205**, 1386–1392 (2010).
[12]. Y. Liao, Y. Zhou, Y. Huang, L. Jiang, Measuring elastic–plastic properties of thin films on elastic–plastic substrates by sharp indentation, *Mechanics of Materials*, **41**, 308–318 (2009).
[13]. R. Araújo, A. M. S. Dias, G. C. D. Godoy, Numerical Study of the Influence of Friction Coefficient for Hardness Testing in Thin Films, *Matéria, in press* (2012) [in Portuguese]
[14]. MARC™, Version 2010, MscSoftware Inc, USA, "Volume A: Theory and User Information", *Users Manual*..
[15]. R. D. Mancosu, in: Recobrimento Tribológico Cr-N e nitretação a Plasma para Melhoria da Resistência à Erosão Cavitacional de um Aço Carbono ABNT 1045: Uma Abordagem Topográfica, 335p (*PhD Thesis, Federal University of Minas Gerais, 2005*). [in Portuguese]
[16]. J. E. Shigley: *Mechanical Engineering Design*, McGraw Hill, Eighth Edition, Singapore, 1058p (2006).